



Structural Diversities in Metal-Organic Coordination Polymers Based on Flexibility in Organic Spacer

Anindita Chakraborty and Tapas Kumar Maji*

Abstract | Metal-organic coordination polymers with their various novel structural motifs have drawn intense research interests over the last few decades. Interestingly, flexibility of the organic spacers in such metal-organic coordination polymers can direct various structural topology and intricate networks. A novel 1D coordination polymer and some other illustrative examples with different flexible ligands like 1,2-bis(4-pyridyl)ethane (bpe) and 1,3-bis(4-pyridyl)propane (bpp) have been discussed in this review. Both *gauche* and *anti*-conformations could be adopted by the bpe ligand, and hence diverse structures can be furnished. Further flexibility could be achieved by exploiting longer ligand like 1,3-bis(4-pyridyl)propane (bpp). Our group has been pursuing research to furnish such flexible compounds and study their different functionalities. An account of design of such diverse systems by employing judicious ligand design strategy and their different structural aspects will be presented in this review.

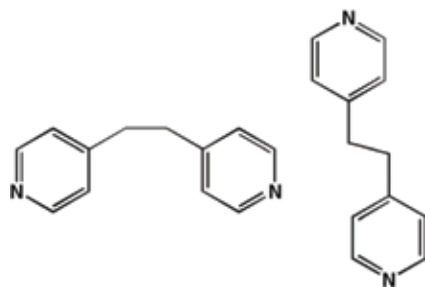
1 Introduction

Research over the past few decades into metal-organic coordination polymers has culminated in the fabrication of new functional materials with interesting structural topologies.¹ Specially the discrete coordination clusters and one-dimensional chains have attracted intense research interest as they are potential candidates for low dimensional magnetic materials.² On the other hand, higher dimensional porous frameworks are useful as potential candidates for gas adsorption study.³ These various coordination architectures also deserve special research interest from the structural point of view. Chemists have been involved in furnishing such new compounds which could be entirely characterized by single-crystal X-ray crystallography. However, synthesis of these desired compounds is not always straightforward and requires rational synthetic strategy. Self-assembly between metal ions and proper organic linkers have often been employed to synthesise versatile metal-organic coordination polymers.¹ Several factors like coordination geometry of the metal ion, structure and flexibility of the ligand and reaction conditions govern the final structure of

the resulting compound. Flexibility is one important aspect of the organic spacer system which can eventually result in flexible materials that are potential candidates for showing various guest-dependent behaviours.⁴ The choice of ligand is very crucial for the design of desired molecular architecture. The 1,2-bis(4-pyridyl)ethane (bpe)⁵ ligand can bind metal ions in different ways and it has widely been exploited in coordination chemistry as a spacer for the construction of extended framework system.⁶ Moreover, this versatile ligand can also adopt different conformations like *gauche* and *anti* conformations,⁷⁻⁹ the former being rarely explored (Scheme 1). In this review, we discuss some of the illustrative literature reports showing such conformational flexibilities. Along with the discussion of the reported structures, we also report herein synthesis and single-crystal structural characterization of a new one-dimensional metal-organic coordination polymer $\{[\text{Co}(\text{bpe})_2(\text{Cl})(\text{H}_2\text{O})]\text{Cl}\cdot 2\text{H}_2\text{O}\}$ (1). 1 contains one-dimensional chains and cationic channels formed by these chains. These channels are occupied by non-coordinated chloride anions and guest water molecules. Since the framework

Molecular Materials
Laboratory, Chemistry and
Physics of Materials Unit,
Jawaharlal Nehru Centre
for Advanced Scientific
Research, Jakkur,
Bangalore 560 064, India.

*tmaji@jncasr.ac.in



Scheme 1: A Scheme showing the two different conformation of bpe ligand: (a) *syn* and (b) *anti* conformations. The *syn* conformation is relatively less exploited in the supramolecular structures.

has free anions in the channels, it can be utilized for selective anion exchange with other anions based upon their size and charge as previously demonstrated by our group.¹⁰

In the recent past, our group also furnished various other coordination polymers having both *gauche* and *anti* conformations of the bpe ligand. Such illustrative examples will be discussed in this review. Being a long organic ligand, bpe can afford interpenetrated structure, which was realized by our group through fabrication of a 3-fold interpenetrated framework $\{[\text{Cu}(\text{bpe})_{0.5}(\text{2,6-ndc})] \cdot 0.5\text{H}_2\text{O}\}_n$ (**2**) (2,6-ndc = 2,6-naphthalenedicarboxylate).^{11a} Furthermore, structural transformation involving dimensionality change with concomitant change from *anti* to *gauche* conformation of bpe has also been reported by our group.¹² We have synthesized 3D frameworks with formula $\{[\text{M}(\text{bpe})_2(\text{N}(\text{CN})_2)_2\text{N}(\text{CN})_2 \cdot x\text{H}_2\text{O}]\}_n$ (M = Zn(II) (x = 5) (**3**)/ Co(II) (x = 4) (**4**) [$\text{N}(\text{CN})_2^-$ = dicyanamide], which undergo structural change upon heating, furnishing 1D coordination chain $[\text{M}(\text{bpe})(\text{N}(\text{CN})_2)_2]_n$ and this change was triggered by conformational flexibility of bpe ligand.¹² Exploitation of even longer ligands like 1,3-bis(4-pyridyl)propane (bpp) led to flexible 2D network with the formula $\{[\text{Ni}(1,3\text{-adc})(\text{bpp})(\text{H}_2\text{O})_2] \cdot (\text{H}_2\text{O}) \cdot (\text{EtOH})\}_n$ (**5**), which showed guest specific adsorption behavior.¹³ Reversible structural dynamism was observed for a flexible 2D bilayer framework $\{[\text{Cu}(\text{pyrdc})(\text{bpp})](5\text{H}_2\text{O})\}_n$ (**6**) [pyrdc = pyridine-2,3-dicarboxylate].¹⁴ The structural aspects of these compounds will be discussed in the following part of this review.

2 Coordination Compound with *Gauche* Conformation of bpe

As we mentioned before, the bpe ligand is a conformationally flexible ligand with the ability to bind metal ions in different fashions (*gauche* and *anti*). Although there are a number of reports with

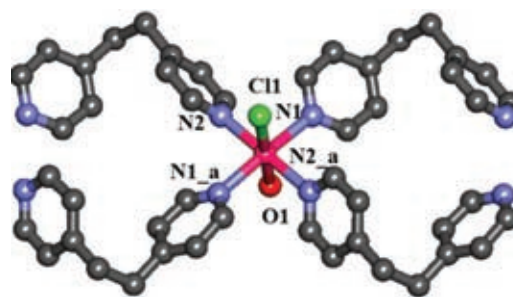


Figure 1: The coordination environment around octahedral Co(II) ion in compound **1**. Symmetry code: a = 1-x, y, 2-z. Colour code: cobalt(II): pink; nitrogen: blue; carbon: grey; oxygen: red; chlorine: green.

the *anti* conformations, the *gauche* conformation has not been very frequently furnished. Here we report a new one-dimensional metal-organic coordination compound $\{[\text{Co}(\text{bpe})_2(\text{Cl})(\text{H}_2\text{O})] \text{Cl} \cdot 2\text{H}_2\text{O}\}$ (**1**), which was synthesized by exploiting self-assembly between CoCl_2 and bpe ligand (1:2 molar ratio) in $\text{H}_2\text{O}/\text{MeOH}$ medium and at room temperature. Compound **1** crystallizes in monoclinic $C2$ space group, and the structure determination by single-crystal X-ray diffraction studies¹⁷ reveals a 1D coordination chain of Co(II), construction of which is facilitated by bridging bpe ligands. In the asymmetric unit, there is a one crystallographically independent Co(II) centre having slightly distorted octahedral coordination geometry (Figure 1, Symmetry codes: a = 1-x, y, 2-z), one bpe ligand, one coordinated and one guest chloride ion and similarly one coordinated and one guest water molecule. The coordination sphere of Co(II) are furnished by two bpe ligands, one coordinated chloride ion and one coordinated water molecule. N1, N2_a and N2, N1_a from two bpe ligands occupy the equatorial positions while O1 from the guest water and Cl1 atom fulfil the axial coordination sites. The equatorial Co–N bond lengths are 2.173(2) Å and 2.179(2) Å; while the axial Co–Cl1 and Co–O1 bond distances are 2.4674(13) Å and 2.101(3) Å, respectively. The bpe ligand binds one Co(II) centre with its symmetry-equivalent counterpart (Co_a; a = 1-x, y, 2-z) in a *syn*-conformation along the crystallographic *c* axis, which results in the formation of an 1D cationic chain (Figure 2).

The adjacent metal centres bridged by the bpe ligands are at a distance of by 9.725 Å. Torsion angle involving the four carbon atoms C3, C6, C7 and C8 is 65.15°, which is a consequence of the *syn* conformation of the bpe ligand. Upon closer analysis of the structure, we found significant C–H \cdots π interaction (Figure 3) between the bpe

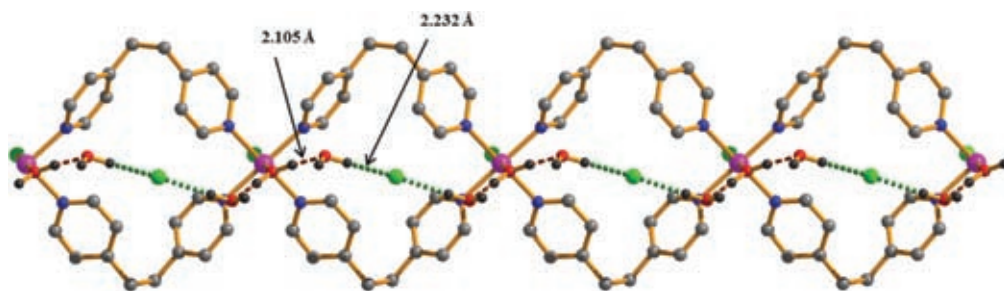


Figure 2: The one-dimensional chain of compound **1** lying along crystallographic *c* axis, where the bpe ligand bridges two Co(II) in syn fashion. The guest water and the counter chloride ion are represented in sphere. Colour code: cobalt(II): pink; nitrogen: blue; carbon: grey; oxygen: red; chlorine: green; hydrogen: black. The H-bonding interaction between coordinated and guest water molecule is shown in brown dotted line and the interaction between guest water and chloride ion is shown in green dotted line.

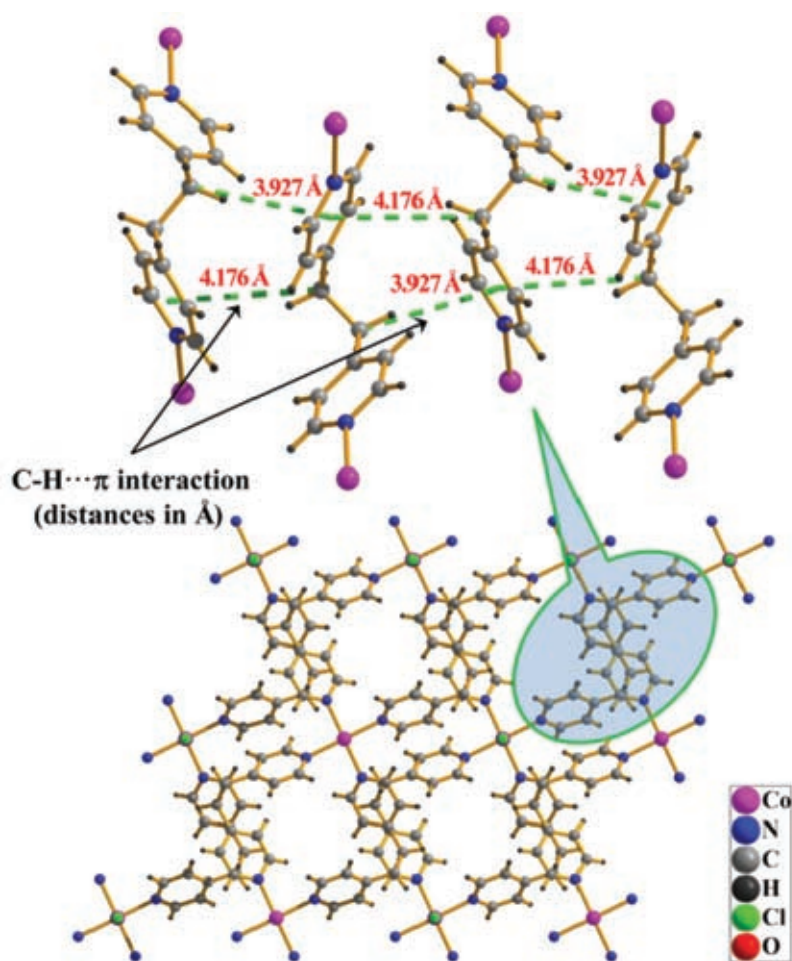


Figure 3: Diagram showing the C-H... π interactions (view along the crystallographic *b* axis) between the bpe ligands in compound **1**.

ligands of neighboring chains, which probably stabilize the supramolecular structure. There are two different kinds of C-H... π interactions, a relatively stronger, C6-HB...cg1, 3.927 Å and another, C7-H7B...cg1, 4.176 Å (cg1 is the centroid formed

by C8, C9, C10, C11, C12 and N1) between the bpe ligands. The stacking of these cationic chains resulting in cationic channels, which are occupied by the guest water molecules and non-coordinated Cl⁻ ions. Along the 1D chain (Figure 4), there is a

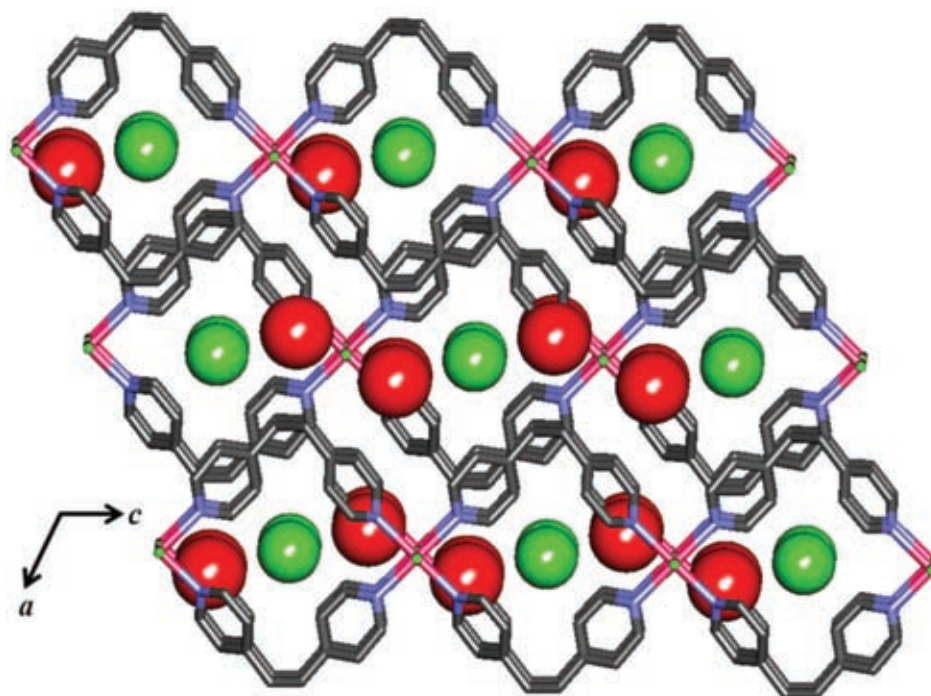


Figure 4: The packing diagram of compound **1** lying along crystallographic *ac* plane. The cationic chains stack together resulting in cationic channels that are occupied by the guest water and counter anions. Colour code: cobalt(II): pink; nitrogen: blue; carbon: grey; oxygen: red; chlorine: green.

strong H-bonding interaction between the coordinated water molecule (O1) and the lattice water molecule (O1w) [O1---O1w = 2.73 Å]. There is also considerable interaction between the guest water molecule (O1w) and the counter chloride anion (Cl2) [Cl2---O1w = 3.15 Å], probably arising because of the halogen bonding.¹⁵

3 Interpenetrated Framework with *anti* Conformation of bpe

A 3-fold interpenetrated 3D framework, $\{[\text{Cu}(\text{bpe})_{0.5}(\text{2,6-ndc})]\cdot 0.5\text{H}_2\text{O}\}_n$ (**2**) (2,6-ndc = 2,6-naphthalenedicarboxylate)^{11a} was designed by our group in recent past. This framework was furnished with the aim for a fabrication material possessing the ability of enhanced H_2 uptake. Interpenetrated frameworks are good candidates for gas adsorption since they can often offer structural rigidity and permanent porosity. Moreover, the interaction between hydrogen molecules and the framework can be enhanced by entrapment mechanism in which a hydrogen molecule would be in close proximity with abundant aromatic rings of interpenetrating frameworks. As suggested by computational study by Zhong and co-workers, another way to establish the strengthened interaction with H_2 molecule is to furnish secondary building units (SBUs) made of metal-oxygen cluster.^{11b} Thus, a reaction strategy

was perceived to blend interpenetration and paddle wheel building units with metal-oxygen cluster in a single framework.

Reaction of Cu(II) with 2,6-ndc yielded $\text{Cu}_2(\text{CO}_2)_4$ paddlewheel building blocks. These paddle-wheel cores are linked together by 2,6-ndc ensuing a 2D infinite grid in the crystallographic *ab* plane. The 2D nets are further connected by bpe linker, resulting a α -Po type 3D framework of **2**. Interestingly, bpe is present in *anti* conformation in this compound, unlike compound **1**. The flexible longer ligand bpe indeed helps to establish flexibility and interpenetration in the resulting framework. The Cu(II) center in asymmetric unit of **2** locates itself with distorted octahedron geometry with $[\text{CuO}_4\text{NCu}]$ chromophore (Figure 5a).

There are two different type of channels, one bilateral triangular channel (with approximate window dimensions $3.4 \times 3.1 \text{ \AA}^2$) along crystallographic [101] direction filled with guest water molecules (Figure 6) and a rectangular channel ($5.8 \times 2.3 \text{ \AA}^2$) along crystallographic *c* direction. There are three structurally different 3D nets resulting from the 3-fold interpenetration in the framework (Figure 5c). The nearest Cu...Cu distance along Cu...2,6-ndc...Cu and Cu...bpe Cu distances are 13.005 Å and 13.556 Å, respectively. The dehydrated compound undergoes structural

change as a result of flexibility of the bpe ligand. The (11 $\bar{1}$) peak in **2** is shifted to higher angle in dehydrated framework (Figure 7). This plane indeed contains flexible $-\text{CH}_2-\text{CH}_2-$ part of the

bpe ligand, and after the loss of crystalline water molecules, rearrangement of the bpe linker in the (11 $\bar{1}$) plane ensues this change. The dehydrated framework also showed interesting adsorption behaviour.

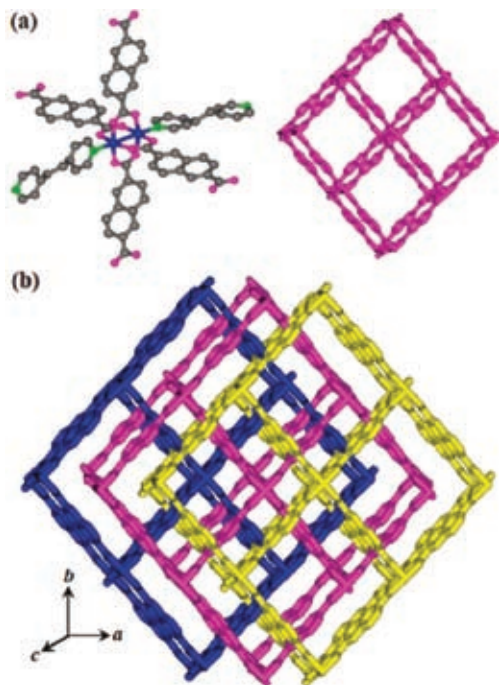


Figure 5: Crystal structure of **2**: (a) left, coordination environment of Cu(II) (Colour code: copper, blue; oxygen, pink; nitrogen, green; carbon, gray); right, simplified view of a single net in **2**. (b) View of the 3D α -Po type 3-fold interpenetrated framework along crystallographic c direction (hydrogen atoms are removed for clarity). Reprinted (adapted) with permission from reference 11a. Copyright 2009, American Chemical Society.

4 Single-Crystal to Single-Crystal Transformation from 3D Framework to 1D Chain Triggered by Conformational Change of bpe Ligand

One interesting case of crystal-to-crystal transformation of two isostructural 2-fold interpenetrated α -polonium type 3D porous coordination frameworks, $\{[\text{M}(\text{bpe})_2(\text{N}(\text{CN})_2)]\text{N}(\text{CN})_2 \cdot x\text{H}_2\text{O}\}_n$ ($\text{M} = \text{Zn}(\text{II})$ ($x = 5$) (**3**)/ $\text{Co}(\text{II})$ ($x = 4$) (**4**) [$\text{N}(\text{CN})_2^- = \text{dicyanamide}$].¹² These frameworks showed 3D \rightarrow 1D structural transformation upon loss of one bpe and conformational change from anti to gauche by another bpe ligand. Compounds **3** and **4** both exhibited 3D α -Po type coordination framework of $\text{M}(\text{II})$ [$\text{M} = \text{Zn}(\text{II})$ (**3**)/ $\text{Co}(\text{II})$ (**4**)] connected by bpe and $\text{N}(\text{CN})_2^-$ linkers. Four bpe linkers connected to the $\text{M}(\text{II})$ center result in a 2D network of $\{\text{M}(\text{bpe})_2\}^{2+}$ along the crystallographic ab plane (Figure 8a).

The 2D nets are further pillared by $\text{N}(\text{CN})_2^-$ resulting in a α -polonium type 3D framework. The 3D framework shows 2-fold interpenetration (Figure 8c) with two dissimilar channels; a hexagonal channel having dimension of $5.5 \times 4.5 \text{ \AA}^2$ ($6 \times 4.5 \text{ \AA}^2$ for compound **4**) contains guest water molecules, and another rectangular pore with dimension of $2.0 \times 0.5 \text{ \AA}^2$ ($2.5 \times 0.5 \text{ \AA}^2$, for compound **4**) contains $\text{N}(\text{CN})_2^-$ anions. The bpe ligand is conformationally flexible and is present in *anti* conformation with a dihedral angle of 176.37°

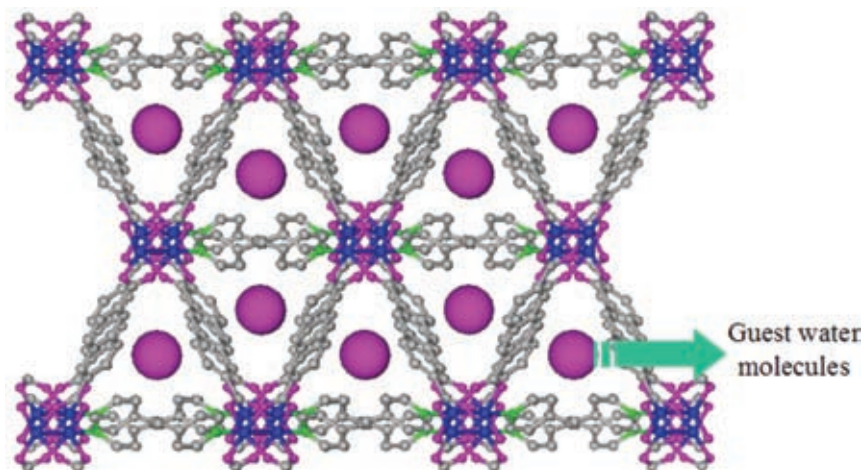


Figure 6: View of the water filled channels of **2** along $[101]$ directions (Colour code: Copper, blue; Oxygen, pink; Nitrogen, green; Carbon, grey). Reprinted (adapted) with permission from reference 11a. Copyright 2009, American Chemical Society.

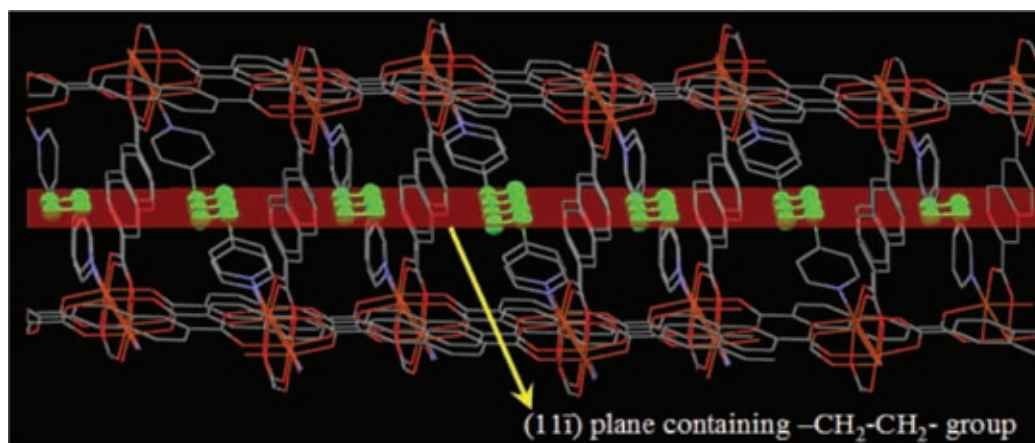


Figure 7: The flexible $-\text{CH}_2\text{CH}_2-$ group in compound **2** is aligned in $(11\bar{1})$ plane which is responsible for structural rearrangement at high temperature. Reprinted (adapted) with permission from reference 11a. Copyright 2009, American Chemical Society.

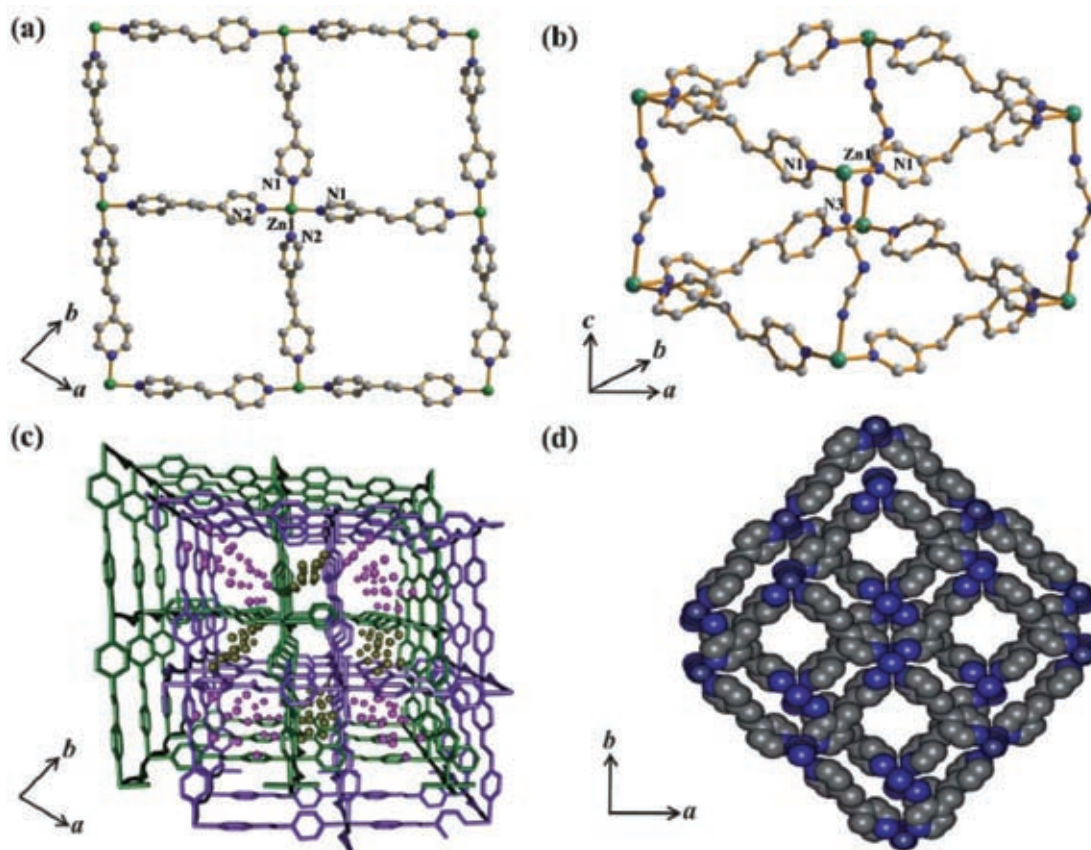


Figure 8: (a) 2D network of $\{\text{Zn}(\text{bpe})_2\}^{2+}$ along crystallographic ab plane, (b) α -Po type 3D building unit. (c) View of 3D framework showing two-fold interpenetrated bimodal channel structure, (d) CPK diagram showing two different types of pores along crystallographic c axis. Reproduced from reference 12 with permission from The Royal Society of Chemistry.

(178.14° for compound **4**) along the ethane C–C bond.

The thermogravimetric (TG) profile (Figure 9) of compound **3** was particularly

interesting which indeed prompted us to carry out single-crystal to single-crystal structural transformation experiment. In the temperature range $30\text{--}75^\circ\text{C}$, the guest water molecules

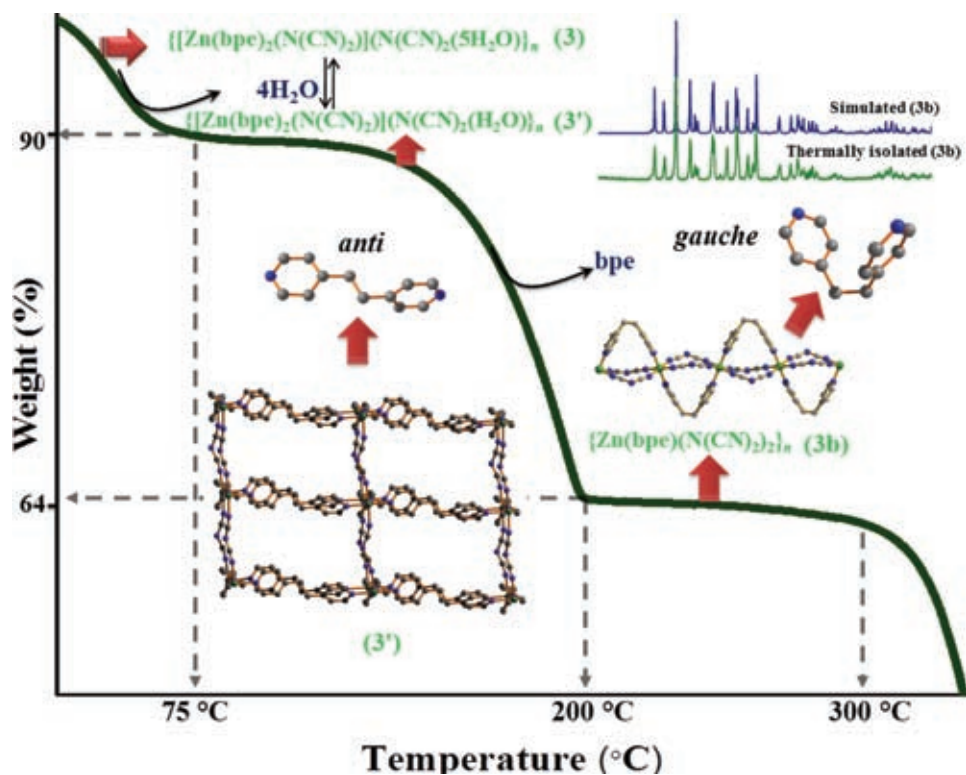


Figure 9: Schematic representation of 3D $\{[\text{Zn}(\text{bpe})_2(\text{N}(\text{CN})_2)(\text{N}(\text{CN})_2 \cdot 5\text{H}_2\text{O})]_n\}$ (**3**) to 1D $\{[\text{Zn}(\text{bpe})(\text{N}(\text{CN})_2)_2]_n\}$ (**3b**) crystal-to-crystal transformation triggered by release of the one coordinated bpe linker; PXRD pattern of thermally isolated product and as-synthesized compound and the 1D coordination chain of $\{[\text{Zn}(\text{bpe})(\text{N}(\text{CN})_2)_2]_n\}$. Reproduced from reference 12 with permission from The Royal Society of Chemistry.

are lost and the dehydrated framework is stable upto 145 °C. Subsequent weight loss in the range 150–200 °C corresponded to loss of one bpe ligand. The other bpe ligand is lost at around 340 °C. A partially dehydrated single-crystal structure $\{[\text{Zn}(\text{bpe})_2(\text{N}(\text{CN})_2)](\text{N}(\text{CN})_2 \cdot \text{H}_2\text{O})_n\}$ was obtained, which showed overall preservation of the as-synthesized 3D structure of **3**. Upon rehydration, the parent structure could be regenerated, thus suggesting a reversible single-crystal to single-crystal transformation. By heating compound **3** and **4** at 200 °C under vacuum for 6 hours, distinct colour change (white to light brown for **3** and orange to red for **4**) was obtained due to the loss of one bpe ligand. The structure was formulated as $[\text{M}(\text{bpe})(\text{N}(\text{CN})_2)_2]_n$ as proposed by elemental analysis results. Single-crystals were separately prepared following the same composition and structure determination suggests that **3b** and **4b** are 1D coordination chains bridged by two $\text{N}(\text{CN})_2^-$ anions and one bpe ligand present in a *gauche* conformation connecting the M(II) centers. To best of our knowledge, such 3D→1D structural change triggered by conformational change of bpe is unprecedented.

5 Flexible Framework with 1,3-bis(4-pyridyl)propane (bpp) Ligand

We recently reported a mixed-ligand PCP, $\{[\text{Ni}(1,3\text{-adc})(\text{bpp})(\text{H}_2\text{O})_2] \cdot (\text{H}_2\text{O}) \cdot (\text{EtOH})\}_n$ (**5**) which was constructed from flexible organic linkers, 1,3-*adc* and *bpp*, (1,3-*adc* = 1,3-adamantanedicarboxylate; *bpp* = 1,3-bis(4-pyridyl) propane) at RT. Ni(II) and 1,3-*adc* ligand form 1D chains along *c* direction and are connected by the *bpp* linkers to generate a 2D triangular corrugated layer in the crystallographic *ac* plane (Figure 10a). The 2D corrugated layers stack in AB fashion along *b* direction and are interdigitated (Figures 10b). This interdigitation is supported by H-bonding and hydrophobic interactions resulting in the formation of a 3D supramolecular framework (Figures 11). The 3D supramolecular framework provides 1D dumbbell shaped channels of dimension $5.4 \times 2.0 \text{ \AA}^2$ along *b* axis and are occupied by the guest water and EtOH molecules. The desolvated compound provides 22.12% void volume per unit cell volume. The flexibility of the spacer (*bpp*) is reflected in the framework structure too and consequently, the desolvated framework, $\{[\text{Ni}(1,3\text{-adc})(\text{bpp})]\}_n$ undergoes structural transformation. Structural

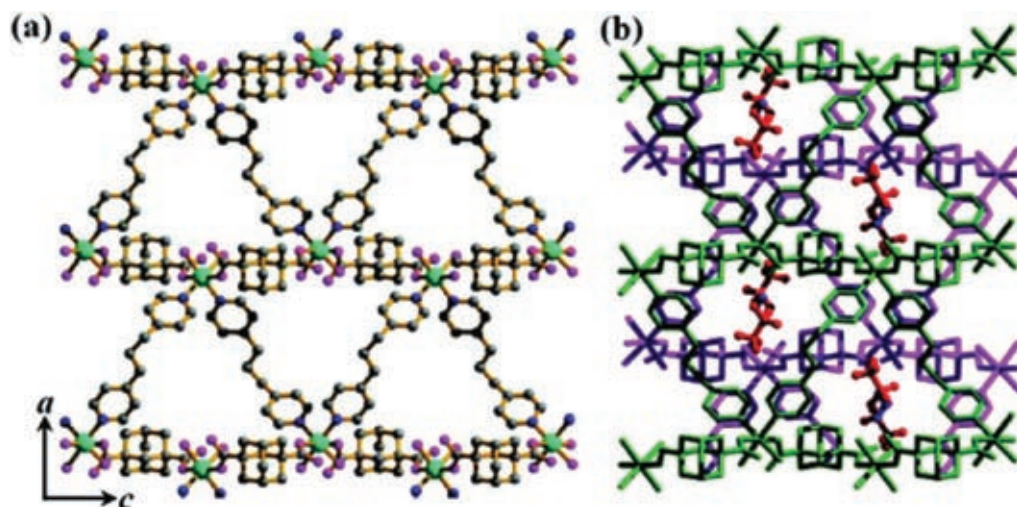


Figure 10: (a) 2D triangular sheet of **1** composed of 1D $[\text{Ni}(1,3\text{-adc})]_n$ chains connected by the bpp linker; (b) 2D sheets stack along the b axis in AB fashion forming 1D channels occupied by H_2O (blue) and EtOH (red) molecules. Reprinted (adapted) with permission from reference 13. Copyright 2011, American Chemical Society.

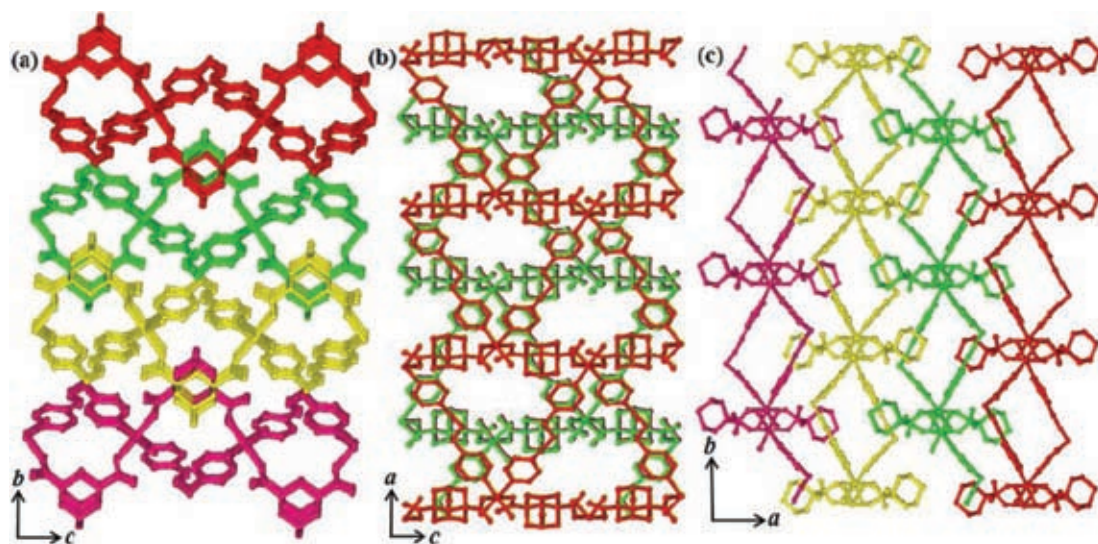


Figure 11: Packing of the 2D corrugated sheet of compound **5**: (a) along crystallographic a -axis interdigitated in between 1,3-*adc* linker with hydrophobic interactions; (b) along b -axis ABAB stacking provide 1D channels occupied by the guest H_2O and EtOH molecules; (c) along c -axis. Reprinted (adapted) with permission from reference 13. Copyright 2011, American Chemical Society.

contraction was evident and the desolvated compound was found to display double-step hysteretic profiles for CO_2 , H_2O , MeOH and a single-step gate opening behavior with EtOH. Each step of MeOH adsorption was monitored with powder X-ray diffraction (PXRD) experiment.

6 2D Bilayer Open Framework with bpp Ligand

2D pillared-bilayer framework could be furnished exploiting mixed ligand. A Cu(II)-based

framework $\{[\text{Cu}(\text{pyrdc})(\text{bpp})](5\text{H}_2\text{O})\}_n$ (**6**) (pyrdc = pyridine-2,3-dicarboxylate; bpp = 1,3-bis(4-pyridyl)propane) was synthesized which crystallized in a pillared-bilayer 2D framework¹⁴ where the 2D layer exhibited a honeycomb motif consisting of $\text{Cu}(\text{pyrdc})(\text{bpp})$ (Figure 12). One remarkable feature of this compound is the binding of the bpp spacer. The pyridine- $(\text{CH}_2)_3$ - fragment of bpp shares a part of a 2D layer and the remaining pyridine part of the bpp joins the other layer, thus ensuring a pillared-bilayer structure.

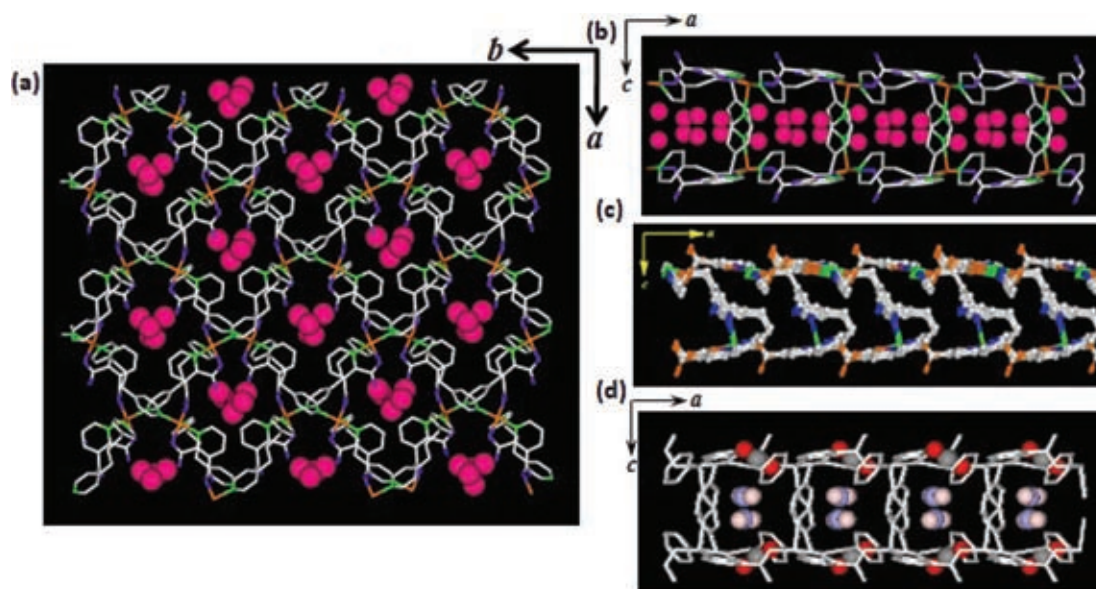


Figure 12: (a) Honeycomb-like 2D layer of $\{[\text{Cu}(\text{pyrdc})(\text{bpp})](5\text{H}_2\text{O})\}_n$ filled with guest H_2O molecules along the c -axis; (b) pillared-bilayer network along the b -axis with H_2O molecules; (c) honeycomb-like 2D layers of desolvated framework; (d) pillared-bilayer network along the b -axis with CO_2 molecules. Reprinted (adapted) with permission from reference 14. Copyright 2005, American Chemical Society.

An unusual bent conformation of the bpp was observed along the alkyl chain $-(\text{CH}_2)_3-$ resulting in the formation of pillared-bilayer structure of this framework.

The alkyl chain is in a bending conformation with the angle, py-C-C of 111.50° , while the two pyridine rings are in *anti* conformation with dihedral angle of $70.2(5)^\circ$. Along the crystallographic c and b axis, the channels dimensions are $5.5 \times 3.7 \text{ \AA}^2$ and $2.3 \times 2.1 \text{ \AA}^2$ respectively, and these are occupied by guest water molecules. Single-crystal-to-single-crystal structural transformation is exhibited by the dehydrated framework and a new non-porous phase with the molecular formula $\{[\text{Cu}(\text{pyrdc})(\text{bpp})]_2\}_n$ is obtained, where one detached pyridine part from $\text{Cu}(\text{II})$ occupies the void space. This nonporous compound does not uptake N_2 or O_2 , but adsorbs an unusually high amount of CO_2 at 195 K. Furthermore, the CO_2 included single crystal structure was also determined, which reveals a structure similar to the as-synthesized framework with the regeneration of the $\text{Cu}(\text{II})$ -N bond with bpp. In the micropores, CO_2 molecules are adsorbed and undergo several $\text{C-H}\cdots\text{O}$ hydrogen bonding interactions, which are not feasible for N_2 or O_2 . This ushers selective CO_2 inclusion, and such selectivity is driven by the interactions with the pillar modules.

7 Conclusion

Flexibility in organic spacers plays a crucial role in furnishing flexible metal-organic architecture, which eventually affects the properties of these

architectures. We have discussed here the diverse structural aspects of metal-organic coordination compounds with two organic spacers, namely 1,2-bis(4-pyridyl)ethane (bpe) and 1,3-bis(4-pyridyl)propane (bpp). These ligands show conformational flexibility, which is reflected in the diverse structures of the resulting compounds. By judicious choice of the ligand systems, different interesting metal-organic compounds can thus be generated, where the structural flexibility of the system will lead to fascinating material properties like guest-dependent structural change and corresponding alteration in adsorption, luminescence and magnetic property.

Acknowledgements

Authors are grateful to Department of Science and Technology, Government of India for the financial support. TKM acknowledges Sheikh Saqr fellowship.

Received 3 November 2013.

References

- (a) A. K. Cheetham and C. N. R. Rao, *Science* 2007, 318, 58;
 (b) J. R. Long, O. M. Yaghi, *Chem. Soc. Rev.* 2009, 38, 1213;
 (c) O. M. Yaghi, M. O'Keeffe, N. W. Ockwig, H. K. Chae, M. Eddaoudi and J. Kim, *Nature* 2003, 423, 705;
 (d) K. L. Gurunatha, G. Mostafa, D. Ghoshal and T. K. Maji, *Cryst. Growth Des.*, 2012, 10, 2483;
 (e) K. L. Gurunatha and T. K. Maji, *Inorg. Chem.*, 2009, 48, 10886;
 (f) D. Ghoshal, T. K. Maji, G. Mostafa, T.-H. Lu and N. Ray Chaudhuri, *Crys. Growth Des.*, 2003, 3, 9.

2. (a) T. C. Stamatatos, A. G. Christou, C. M. Jones, B. J. O'Callaghan, K. A. Abboud, T. A. O'Brien, and G. Christou, *J. Am. Chem. Soc.*, 2007, 129, 9840;
- (b) D. Ghoshal, A. D. Jana, T. K. Maji and G. Mostafa, *Inorg. Chim. Acta*, 2006, 359, 690;
- (c) J. J. Vittal, *Coord. Chem. Rev.*, 2007, 251, 1781;
- (d) C. F. Lee, D. A. Leigh, R. G. Pritchard, D. Schults, S. J. Teat, G. A. Timco and R. E. P. Winpenny, *Nature*, 2009, 458, 314;
- (e) S. Sain, T. K. Maji, D. Das, J. Cheng, T.-H. Lu, J. Ribas, M. Salah El Fallah and N. Ray Chaudhuri, *Dalton Trans.*, 2002, 1302;
- (f) O. Kahn, *Molecular Magnetism*. VCH, New York, 1993;
- (g) P. S. Mukherjee, T. K. Maji, T. Mallah, E. Zangrando, L. Randaccio and N. Ray Chaudhuri, *Inorg. Chim. Acta*, 2001, 315, 249;
- (h) T. K. Maji, I. R. Laskar, G. Mostafa, A. J. Welch, P. S. Mukherjee and N. Ray Chaudhuri, *Polyhedron*, 20, 651, 2001;
- (i) A. Chakraborty, K. L. Gurunatha, A. Muthulakshmi, S. Dutta, S. K. Pati and T. K. Maji, *Dalton Trans.*, 2012, 41, 5879;
- (j) A. Chakraborty, B. K. Ghosh, J. R. Arino, J. Ribas, and T. K. Maji, *Inorg. Chem.*, 2012, 51, 6440;
- (k) A. Chakraborty, L. S. Rao, A. K. Manna, S. K. Pati, J. Ribas and T. K. Maji, *Dalton Trans.*, 2013, 42, 10707.
- (l) K. L. Gurunatha and T. K. Maji, *Inorg. Chem.*, 2009, 48, 10886.
3. (a) P. Kanoo and T. K. Maji, *Eur. J. Inorg. Chem.* 2010, 3762;
- (b) A. Hazra, S. Bonakala, S. K. Reddy, S. Balasubramanian, and T. K. Maji, *Inorg. Chem.*, 2013, 52, 11385;
- (c) A. Chakraborty, R. Haldar and T. K. Maji, *Cryst. Growth Des.*, 2013, 13 (11), 4968;
- (d) A. Hazra, K. L. Gurunatha and T. K. Maji, *Cryst. Growth Des.*, 2013, 13 (11), 4824;
- (e) P. Kanoo, A. C. Ghosh, S. T. Cyriac, T. K. Maji, *Chem. Eur. J.*, 2012, 18, 237;
- (f) K. Jayaramulu, S. Reddy, A. Hazra, S. Balasubramanian and T. K. Maji, *Inorg. Chem.*, 2012, 51, 7103.
4. (a) P. Kanoo, R. Matsuda, Ryo Kitaura, S. Kitagawa, and T. K. Maji, *Inorg. Chem.*, 2012, 51 (17), 9141;
- (b) P. Kanoo, K. L. Gurunatha and T. K. Maji, *J. Mater. Chem.*, 2010, 20, 1322.
5. (a) J. S. Seo, D. Whang, H. Lee, S. I. Jun, J. Oh, Y. J. Jeon and K. Kim, *Nature*, 2000, 404, 982;
- (b) E. Suresh and M. M. Bhadbhade, *CrystEngComm*, 2001, 13, 1.
6. M. Fujita, Y. J. Kwon, M. Miyazawa and K. Ogura, *J. Chem. Soc., Chem Commun.*, 1994, 1977.
7. T. L. Hennigar, D. C. MacQuarrie, P. Losier, R. D. Rogers and M. J. Zaworotko, *Angew. Chem., Int. Ed.*, 1997, 36, 972.
8. M. Fujita, S. Nagao, M. Iida, K. Ogata and K. Ogura, *J. Am. Chem. Soc.*, 1993, 115, 1574.
9. M. Ferbinteanu, G. Marinescu, H. W. Roesky, M. Noltemeyer, H. G. Schmidt and M. Anruth, *Polyhedron*, 1998, 18, 243.
10. S. Y. Vyasamudri and T. K. Maji, *Chem. Phys. Lett.*, 2009, 473, 312.
11. (a) P. Kanoo, R. Matsuda, M. Higuchi, S. Kitagawa and T. K. Maji, *Chem. Mater.* 2009, 21, 5860;
- (b) Q. Yang and C. Zhong, *J. Phys. Chem. B*, 2006, 110, 655.
12. R. Haldar and T. K. Maji, *CrystEngComm*, 2012, 14, 684.
13. P. Kanoo, R. Sambhu and T. K. Maji, *Inorg. Chem.*, 2011, 50, 400.
14. T. K. Maji, G. Mostafa, R. Matsuda and S. Kitagawa, *J. Am. Chem. Soc.*, 2005, 127, 17152.
15. R. Bertani, P. Sgarbossa, A. Venzo, F. Lelj, M. Amati, G. Resnati, T. Pilati, P. Metrangolo and G. Terraneo, *Coord. Chem. Rev.*, 2010, 254, 677.
16. Crystallographic data for compound **1**: Crystal system: Monoclinic, Empirical formula: $C_{24}H_{30}CoN_4Cl_2O_3$; a (Å): 16.0837(9); b (Å): 8.9943(4); c (Å): 9.7251(4); β (°): 110.924(2); V (Å³): 1314.07(11); Z : 2; R : 0.0382; R_w : 0.0651 [$R = \frac{\sum |F_o| - |F_c|}{\sum |F_o|}$]. $R_w = [\frac{\sum \{w(F_o^2 - F_c^2)\}}{\sum \{w(F_o^2)\}}]^{1/2}$.



Anindita Chakraborty completed graduation (B.Sc. in Chemistry) from Presidency College, Kolkata in 2009 and masters (MS in materials science) from Jawaharlal Nehru Centre for Advanced Scientific Research (JNCASR) in 2012. She is currently pursuing her research as an integrated Ph.D. student under the supervision of Prof. Tapas Kumar Maji, in Chemistry and Physics of Materials Unit (CPMU) of JNCASR. Her research works focuses on fabrication of functional metal-organic coordination compounds and study of their magnetism, adsorption and luminescence properties.



Tapas Kumar Maji obtained his Ph.D. in 2002 from Indian Association for the Cultivation of Science (IACS), Kolkata. After a postdoctoral stint at Kyoto University with Prof. Susumu Kitagawa, he joined in Jadavpur University. Then he moved to Jawaharlal Nehru Centre for Advanced Scientific Research (JNCASR), Bangalore. Currently he is an associate professor of Chemistry and Physics of Materials Unit at JNCASR. His current research interest is the development of energy and environment related materials based on functional Metal-Organic Frameworks (MOFs) and Organic Porous Polymers in bulk and nanoscale. He is also involved in synthesis of luminescent and magnetic MOF materials.